Bioorganic & Medicinal Chemistry Letters 21 (2011) 670–676

Contents lists available at ScienceDirect

Bioorganic & Medicinal Chemistry Letters

journal homepage: www.elsevier.com/locate/bmcl

Tetrahydroquinoline derivatives as opioid receptor antagonists

Cunyu Zhang [a,*], Susan M. Westaway [b], Jason D. Speake [a,†], Michael J. Bishop [a], Aaron S. Goetz [c], Luz Helena Carballo [c], Mike Hu [d], Andrea H. Epperly [d]

[a] Department of Medicinal Chemistry, GlaxoSmithKline, Research Triangle Park, NC 27709, USA
[b] Immuno-Inflammation CEDD, GlaxoSmithKline, Gunnels Wood Road, Stevenage SG1 2NY, UK
[c] Molecular Discovery Research, Screening & Compound Profiling, GlaxoSmithKline, Research Triangle Park, NC 27709, USA
[d] Department of Drug Metabolism and Pharmacokinetics, GlaxoSmithKline, Research Triangle Park, NC 27709, USA

ARTICLE INFO

Article history:
Received 12 October 2010
Revised 30 November 2010
Accepted 2 December 2010
Available online 8 December 2010

Keywords:
Tetrahydroquinoline
Opioid
Antagonist

ABSTRACT

Opioid receptors play an important role in both behavioral and homeostatic functions. We herein report tetrahydroquinoline derivatives as opioid receptor antagonists. SAR studies led to the identification of the potent antagonist **2v**, endowed with 1.58 nM (K_i) functional activity against the μ opioid receptor. DMPK data suggest that novel tetrahydroquinoline analogs may be advantageous in peripheral applications.

Opioid receptors belong to the super family of G protein-coupled receptors and are involved in multiple physiological activities, including pain management, reward mechanisms, GI motility, hormone release, and eating behavior.[1] There are three major opioid receptor subtypes: μ, κ and δ, with variant functions and tissue distribution. Humans have many endogenous peptide ligands for opioid receptors, including the well-known endorphins and enkephalins. While opioid agonists, such as morphine (Fig. 1), are clinically used as analgesics, opioid antagonists have also found a number of therapeutic applications, including treatments for opioid addiction, alcohol dependence, interstitial cystitis and smoking cessation.[2] As early as the 1970s, it was reported that naloxone (Fig. 1), an opioid antagonist, reduced food intake.[3,4] As obesity has reached epidemic level, the investigation of opioid antagonists in controlling body weight has noticeably increased. It has been proposed that blockade of the central opioid pathways by opioid receptor antagonists may represent a potential means to treat human obesity.[5] For example, naltrexone (Fig. 1), a marketed μ opioid antagonist, is being examined in Phase III clinical trial for the treatment of obesity in combination with bupropion.[6,7] LY255582 (Fig. 1), a highly potent pan-opioid antagonist, showed a marked efficacy in reducing food consumption and body weight in an obese animal model.[8,9] Peripheral opioid receptors play a predominant role in the development of opioid bowel dysfunction (OBD). Alvimopan (Fig. 1), a peripherally acting μ opioid antagonist, is used to speed gastrointestinal recovery in patients after abdominal surgery.[10]

Early opioid chemistry work has revealed that the prototypic features in an opioid agonist or antagonist include a substituted basic amine, a phenolic moiety and a carbon skeleton to keep these two points in a certain distance.[11,12] It was further demonstrated that the phenolic hydroxyl could be replaced by a carboxamido group, which was considered as an advantage for better pharmacokinetic properties.[13] After carefully analyzing a number of opioid receptor small molecule ligands including a series of biaryl ethers, such as compound **1** shown on Figure 1,[14,15] we rationalized tetrahydroquinoline derivatives as opioid receptor antagonists (**2**, Fig. 2). In this particular tetrahydroquinoline scaffold, a basic secondary amine with a bulky lipophilic substituent is present, and a benzenecarboxamide has been introduced as a phenol replacement. We here report the synthesis of the novel tetrahydroquinoline analogs and their biological data as opioid antagonists. As part of our investigation on the pharmaceutical values of opioid antagonists, their potential therapeutic application for obesity was preliminarily evaluated.

The initial chemistry to synthesize the proposed tetrahydroquinoline derivatives is illustrated in Scheme 1. Two purchased starting materials, tetrahydroquinoline and 4-bromobenzaldehyde, were coupled under Buchwald condition. The aromatic bromination of compound **3** with *N*-bromosuccinamide (NBS) exclusively occurred on the 6-position. The excellent regioselectivity may be attributed to higher electronic density and less steric hindrance at the

* Corresponding author.
E-mail address: cunyu.a.zhang@gsk.com (C. Zhang).
† Present address: Medicinal Chemistry Department, Targacept Inc., Winston-Salem, NC 27101, USA.

0960-894X/$ - see front matter © 2010 Elsevier Ltd. All rights reserved.
doi:10.1016/j.bmcl.2010.12.010

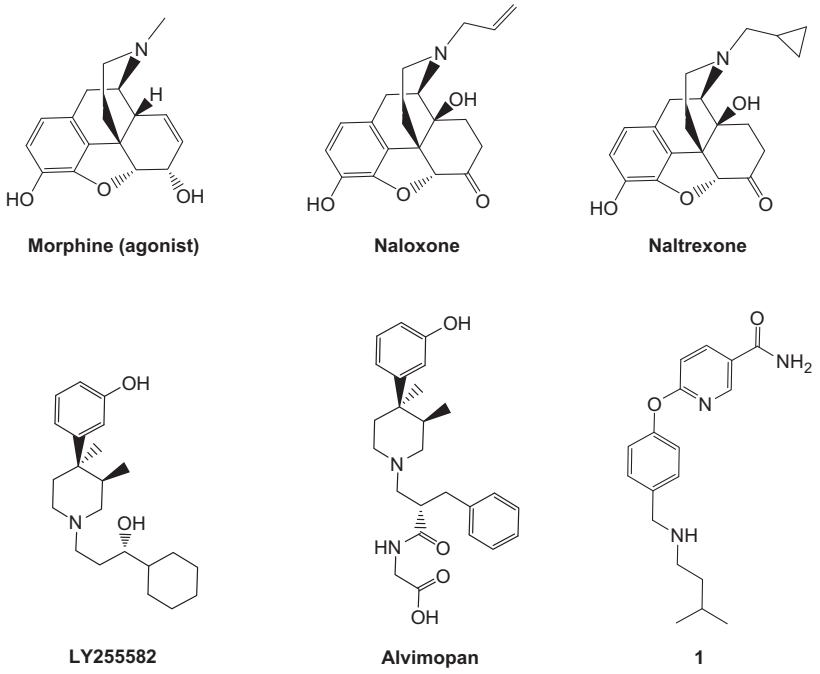

Figure 1. Opiate-acting molecules.

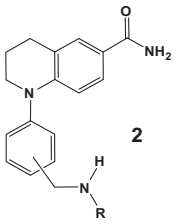

Figure 2.

6-position. The electrophilic substitution took place in DMF at a low temperature although a recent paper reported that a very similar reaction used an ionic liquid in order to achieve a high regioselectivity.[16] Cyanation on compound **4** was fulfilled by a palladium-mediated microwave reaction in 90% isolated yield. Reductive amination of the aldehyde **5** was carried out next, since the nitrile hydrolysis of **5** with hydrogen peroxide could result in the oxidation of the aldehyde functional group. Finally, hydrolysis of compound **6** gave compound **2a** in low yield.

Because the order of the last two steps in the approach shown in Scheme 1 restricted array synthesis of final compounds, an alternative synthetic route was developed (Scheme 2). First, commercially available 6-quinolinecarboxylic acid **7** was partially hydrogenated with ammonium formate in presence of palladium on carbon in a quantitative yield.[17] The acid **8** was converted into methyl ester **9**, followed by Buchwald amination. The aryl amination using the carboxamide version of compound **9** yielded a complicated mixture in which no desired product was isolated. Hydrolysis of the ester **10** with lithium hydroxide then afforded the acid **11**. Due to the presence of the acid-sensitive aldehyde, the mild Vilsmeier reagent, *N*,*N*-dimethylformiminium chloride, was employed to

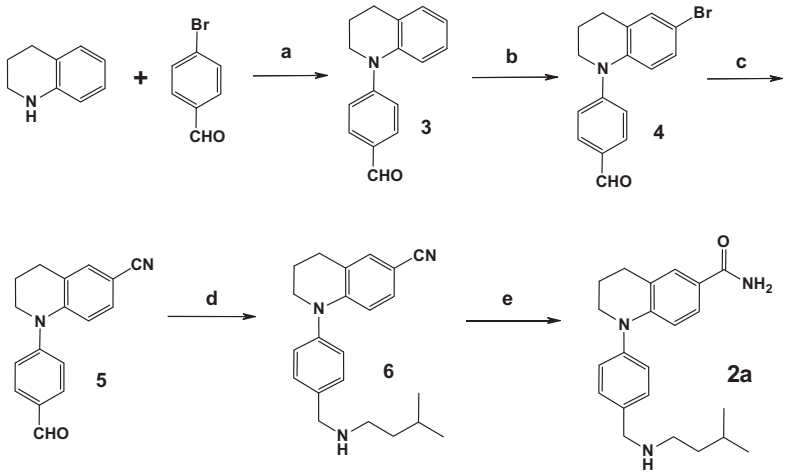

Scheme 1. Reagents and conditions: (a) $Pd(OAc)_2$, BINAP, Cs_2CO_3, toluene, 100 °C, 3 h, 86%; (b) NBS, DMF, −10 °C, 0.5 h, 96%; (c) $Zn(CN)_2$, $Pd(PPh_3)_4$, DMF, 175 °C, MW, 5 min, 90%; (d) isoamylamine (4 equiv), $NaBH(OAc)_3$, MeOH, rt, 83%; (e) 35% H_2O_2, 1 N NaOH, MeOH, rt to 55 °C, 26%.

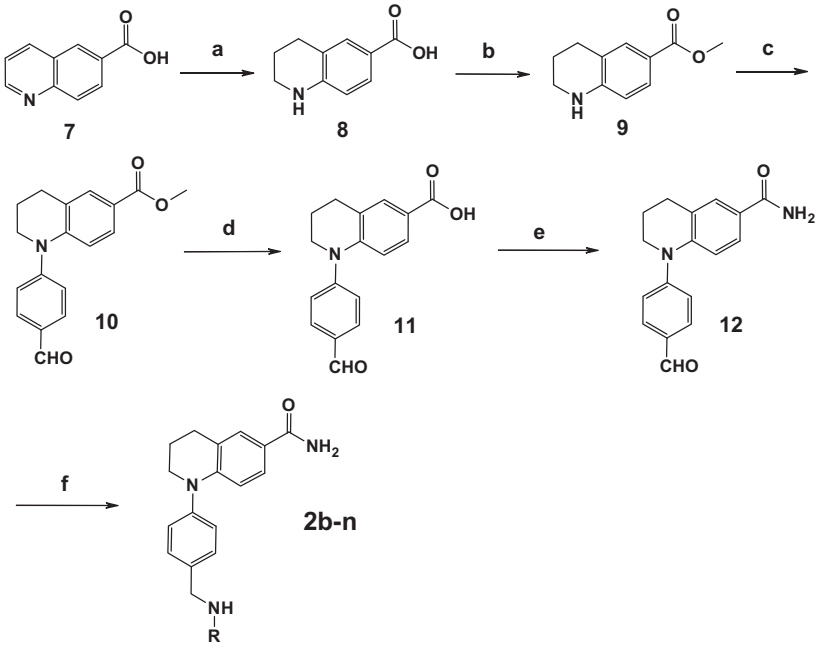

Scheme 2. Reagents and conditions: (a) HCO_2NH_4, 10% Pd/C, MeOH, reflux, 2 h, 100%; (b) thionyl chloride, MeOH, 0 °C to rt,79%; (c) 4-bromobenzaldehyde, $Pd(OAc)_2$, BINAP, Cs_2CO_3, toluene, 100 °C, 10 h, 92%; (d) 2 N LiOH, THF, reflux, 5 h, 88%; (e) $(Me_2N{=}CHCl)Cl$, THF, 0 °C to rt, then 15% aqueous NH_3, 0 °C to rt, 98%; (f) amines (4 equiv), $NaBH(OAc)_3$, MeOH, rt, 70–96%.

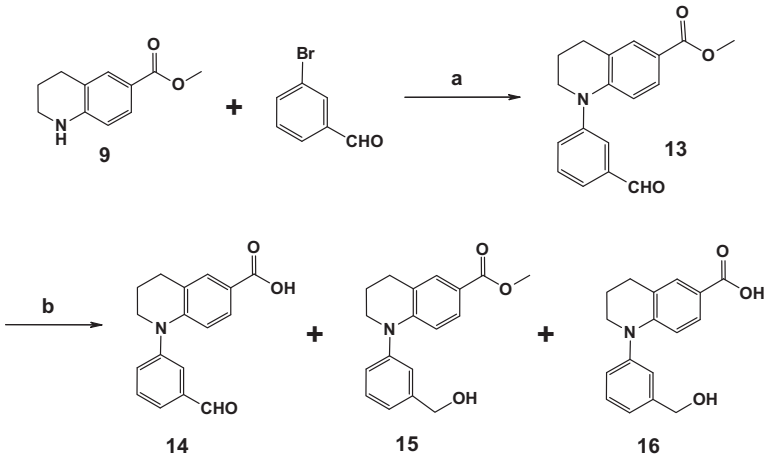

Scheme 3. Reagents and conditions: (a) $Pd(OAc)_2$, BINAP, Cs_2CO_3, toluene, 100 °C, 16 h, 65%; (b) 2 N LiOH, THF, reflux, 18 h.

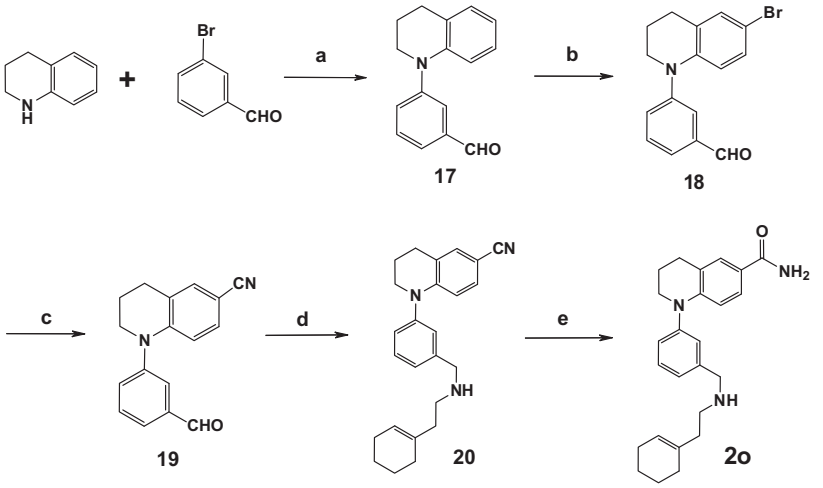

Scheme 4. Reagents and conditions: (a) $Pd(OAc)_2$, BINAP, Cs_2CO_3, toluene, 100 °C, 8 h, 60%; (b) NBS, DMF, −5 °C; (c) $Zn(CN)_2$, $Pd(PPh_3)_4$, DMF, 175 °C, MW, 15 min, 23% in two-steps; (d) 2-(1-cyclohexen-1-yl)ethanamine, $NaBH(OAc)_3$, MeOH, rt; (e) 30% H_2O_2, 5 N NaOH, EtOH, rt to 55 °C, 74% in two-steps.

Table 1
Functional inhibition of human opioid receptors, μ, δ and κ[a]

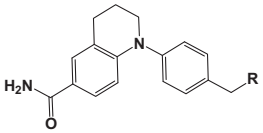

Compound	R	μ, fpK_i [b]	δ, fpK_i	κ, fpK_i
Naltrexone	/	8.70 ± 0.21	7.60 ± 0.22	8.00 ± 0.28
2a	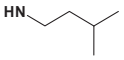	7.10 ± 0.03	6.50 ± 0.48	6.30 ± 0.10
2b		6.20 ± 0.02	<5.40	5.90 ± 0.01
2c	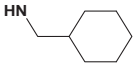	7.40 ± 0.17	6.40 ± 0.06	6.50 ± 0.13
2d	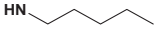	7.30 ± 0.07	6.60 ± 0.14	6.00 ± 0.18
2e	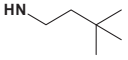	7.30 ± 0.06	6.50 ± 0.18	6.60 ± 0.20
2f	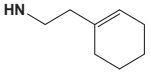	7.60 ± 0.22	6.80 ± 0.16	6.50 ± 0.20
2g	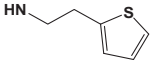	7.60 ± 0.09	6.50 ± 0.22	6.20 ± 0.10
2h	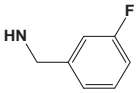	7.00 ± 0.19	6.40 ± 0.25	6.20 ± 0.05
2i	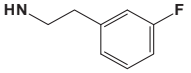	7.50 ± 0.10	6.60 ± 0.11	6.10 ± 0.01
2j	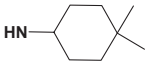	8.00 ± 0.09	7.30 ± 0.29	7.20 ± 0.04
2k	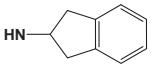	8.30 ± 0.06	7.40 ± 0.12	7.60 ± 0.2
2l	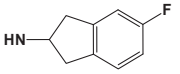	7.90 ± 0.30	7.10 ± 0.11	6.90 ± 0.04
2m	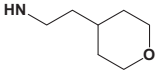	6.90 ± 0.84	6.50 ± 0.27	6.60 ± 0.29
2n	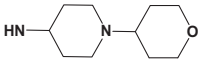	<5.40	<5.40	<5.40

[a] Antagonism of human opioid receptors, μ, δ and κ measured by a GTPgamaS35 LEADseeker bead assay using opioid membranes, hOPRM, hOPRD and hOPRK generated from Bacmam-transduced CHO cells. The constitutive activity was assessed during membrane preparation. An EC_{80} of the agonist was added as the challenge: DAMGO for μ; Met-Enkephalin for δ and Dynorphin A for κ. Assay buffer: 20 mM HEPES, 10 mM $MgCl_2$, and 100 mM NaCl dissolved in lab grade water, pH 7.4 with KOH. For these assays, the typical specific binding ranges from 45–50% of the total. The observed values (ADU) for total and NS binding (total, NS) for μ, δ and κ are: 941, 525; 702, 337; and 692, 376, respectively.

[b] The results were recorded as pIC_{50} values and subsequently converted to fpK_i by the equation: fpK_i = −log(IC_{50}/((2+([L]/EC_{50})^n)^1/n−1)) [L] = concentration of agonist used for antagonist assay; EC_{50} = determined on day of assay using a separate agonist plate containing >6 agonist curves; *n* = slope of agonist curve, mean values: 0.76 (μ), 0.69(δ) and 1.01(κ). For the antagonists tested, mean slope values: 1.13 (μ), 1.03(δ) and 1.02(κ). fpK_i is the negative log of the K_i, thus higher fpK_i indicates a more potent response. The values are the mean of at least two assays. Naltrexone was used as a positive control for each run.

prepare the amide **12** from **11**. A quantitative conversion was achieved. Final reductive amination allowed the attachment of a variety of amines in high yield. Overall, the chemistry depicted in Scheme 2 presented a facile and scalable route to synthesize the desired final compounds.

Final molecules **2a–n** were examined in a [^{35}S]GTPgammaS binding assay,[18] using opioid membranes (hOPRM, hOPRD and hOPRK), generated from Bacmam-transduced CHO cells, to observe functional activity (Table 1). All analogs, except **2n**, showed moderate to high inhibition potency. The indane analog **2k** was the most potent with fpK_i = 8.3 at the μ receptor. Furthermore, all active compounds displayed the strongest inhibition against the μ receptor while the selectivity among the three tested opioid receptors was within a 25-fold range. A few interesting structure–activity relationships were observed: (1) the length of the amine side chain was important (**2a** vs **2b** and **2h** vs **2i**), whereas there was tolerance for size differences at the end of the chain; (2) the side chains having an aromatic moiety were at least as active as the saturated ones; (3) the rigidity in the side chain was usually beneficial for potency (**2i** vs **2l**, e.g.); (4) heteroatoms in the side chains did not improve potency.

In order to further study the substitution pattern for the secondary amine side chain, compound **2o** was synthesized and tested (Table 2). It is worth noting that the general chemistry used for the preparation of *para*-substituted compounds **2b–n** was problematic (Scheme 3) when applied to the synthesis of **2o**. Hydrolysis of ester **13** with LiOH yielded a complicated mixture, in which three major products were formed with only 10–20% each and the desired acid **14** was difficult to isolate. Hence, the approach shown in Scheme 1 was employed to synthesize compound **2o** (Scheme 4). Unfortunately, the yields of several steps were relatively low. The potency of *meta*-substituted analog was two-fold lower at the μ receptor than the corresponding *para* derivative (Table 2, **2f** vs **2o**).

To confirm the importance of the basic nitrogen in the amine side chain, as reported in the literature for opioid agonists,[19] an amide analog **2p** was prepared (Scheme 5) and examined. Its activity significantly dropped on all three opioid receptors, as predicted (Table 2).

With a single digit nanomolar opioid antagonist **2k** (functional K_i = 5.0 nM) in hand, attention turned to optimizing the substitution on the benzyl moiety in the middle. Compounds **2q–x** (Fig. 3) were synthesized using the approach illustrated in Scheme 2. The in vitro receptor inhibition results are summarized in Table 2. The data revealed that all substituents tested at the 3′-postion were detrimental to activity, whether electron donating or withdrawing (**2q** and **2t**). It is likely due to a steric effect of the substitution (**2r** vs **2u**). Moreover, 3′ and 5′-bis-substitution caused a further decrease in activity (**2s**). Nevertheless, the introduction of 2′-methyl did not result in activity drop. It might produce a benefit as compound **2v** was identified as the most potent antagonist in the series so far, with functional pK_i = 8.8. It appears that opioid binding is sensitive to the spatial position of the amine side chain that can be altered by 3′-substitution. However, the opioid receptors tolerate the more twisted middle phenyl portion induced by a 2′-substituent because the amine side chain can correspondingly rotate to the angle to

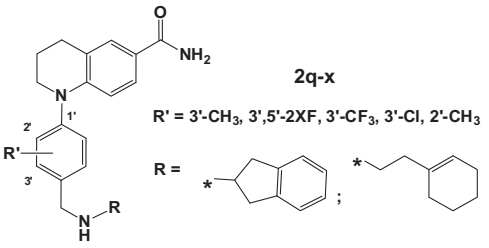

Figure 3.

Table 2
Opioid receptor binding data for further structural modification[a]

Compound	R^1	R^2	μ, fpK_i	δ, fpK_i	κ, fpK_i
2f	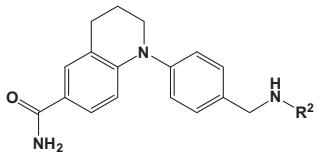	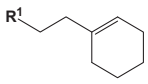	7.60 ± 0.22	6.80 ± 0.16	6.50 ± 0.20
2k	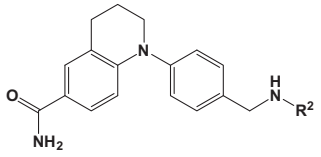	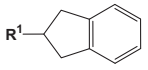	8.30 ± 0.06	7.40 ± 0.12	7.60 ± 0.2
2o	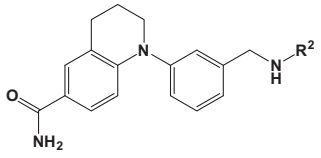	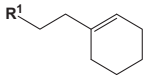	7.30 ± 0.41	6.70 ± 0.01	5.90 ± 0.09
2p	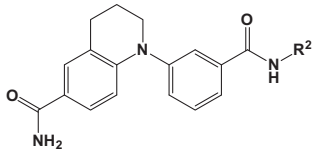	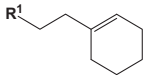	5.70 ± 0.08	5.80	<5.40
2q	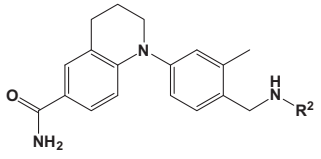	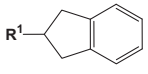	8.10 ± 0.26	6.80 ± 0.07	6.80 ± 0.05
2r	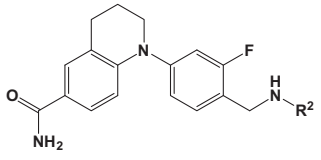	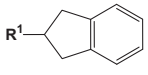	8.10 ± 0.13	7.00 ± 0.05	6.70 ± 0.11
2s	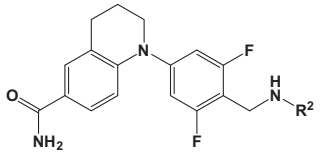	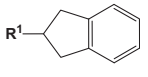	7.60 ± 0.10	6.50 ± 0.32	6.20 ± 0.25
2t	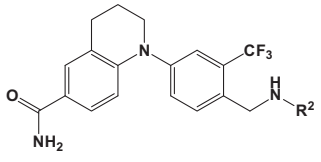	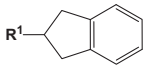	7.30 ± 0.31	7.20 ± 0.97	6.20 ± 0.11
2u	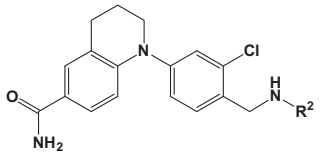	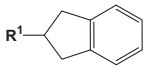	7.80 ± 0.04	7.00 ± 0.06	6.70 ± 0.10
2v	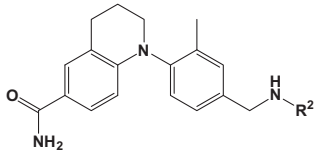	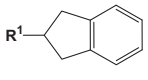	8.80 ± 0.14	7.90 ± 0.27	7.70 ± 0.21

Table 2 (*continued*)

Compound	R^1	R^2	μ, fpK_i	δ, fpK_i	κ, fpK_i
2w	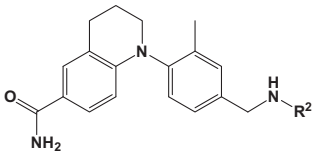	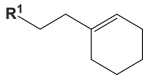	7.90 ± 0.10	7.00 ± 0.32	6.70 ± 0.14
2x	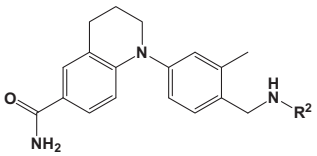	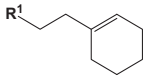	7.00 ± 0.42	6.30 ± 0.36	6.20 ± 0.15
22	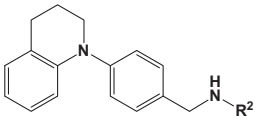	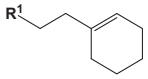	6.40 ± 0.06	<5.40	<5.40
23	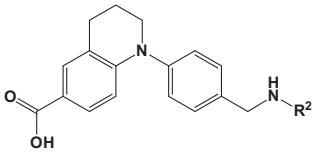	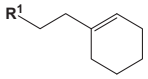	5.50	<5.40	<5.40

[a] Same opioid functional assays were used as Table 1.

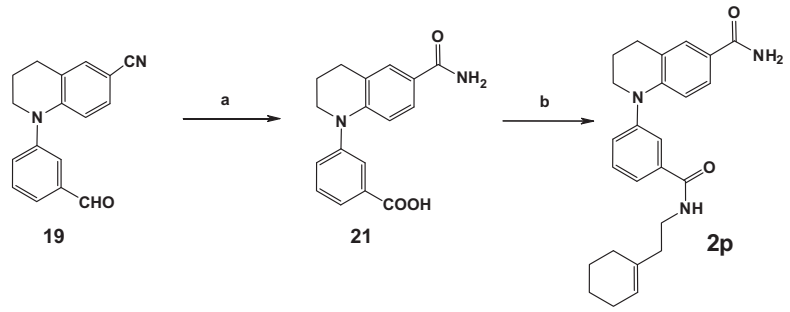

Scheme 5. Reagents and conditions: (a) 30% H_2O_2, 5 N NaOH, EtOH, 55 °C, 18 h, 66%; (b) 2-(1-cyclohexen-1-yl)ethanamine, HBTU, triethylamine, THF/DMF, rt, 100%.

maintain an optimal interaction with the receptor surface. The minor spatial induction may help the binding of the phenylcarboxamide moiety with the opioid receptors as well. The SAR was quite consistent. Just as predicted, the potency of **2w** increased and **2x** dropped, compared to **2f** (Table 2).

We also examined the importance of the carboxamide group on the 6-position. It was found to be critical for this series as the opioid activity of both analogs **22** and **23** dramatically decreased (Table 2). This is consistent with the literature reports that in opioid agonists and antagonists, a phenolic OH or its corresponding bioisostere, such as $CONH_2$, acts as an important H-bond donor for opioid receptor affinity.[13,20,21] Compounds **22** and **23** were synthesized by the methods shown in Scheme 6.

A representative opioid antagonist **2f** was dosed iv in Long-Evans rats to evaluate its pharmacokinetic properties. It exhibited a half life of 5.43 h with moderate volume of distribution (V_{ss} = 1.5 L/kg) and clearance (CL = 26.5 mL/min/kg). Oral dosing determined it had 33% bioavailability, however, its brain to plasma concentration ratio was lower than 0.1. Similar results were observed on other analogs, except having variant bioavailability from 28% to 109%. Although these tetrahydroquinoline analogs had favorable systemic DMPK properties, including good bioavailability, they were not dosed in the feeding study, an initial in vivo pharmacology assay to assess anti-obesity potential, due to poor exposure in the CNS. It is the central opioid system that is involved in the regulation of energy homeostasis.[22] Since poor brain penetration obviously limits the occupancy of central opioid receptors, feeding suppression induced by these tetrahydroquinoline analogs would not be optimal. However, the analogs may find utility in peripheral applications, similar to the marketed medicine, alvimopan.[23]

In summary, we have identified a new structural class of opioid antagonists. Facile syntheses were developed to quickly access these novel tetrahydroquinoline derivatives. The initial SAR study on the amine side chain identified multiple compounds with nanomolar functional activity. Further structural refinement on the middle benzyl moiety helped enhance the opioid activity and led to the discovery of the most potent analog **2v** with functional K_i = 1.58 nM at the μ receptor. In addition, carboxamide proved to be an acceptable hydrogen bond donor in this series. Their unique DMPK properties may offer these opioid antagonists an opportunity in peripheral applications, without affecting central actions of opioid receptors.

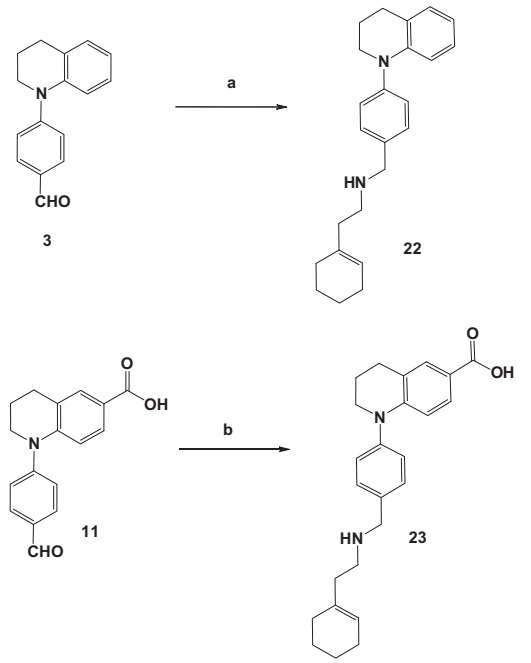

Scheme 6. Reagents and conditions: (a) and (b) 2-(1-cyclohexen-1-yl)ethanamine, $NaBH(OAc)_3$, MeOH, rt.

References and notes

1. Bodnar, R. J. *Peptides* **2009**, *30*, 2432.
2. *Opiate Receptors and Antagonists: From Bench to Clinic*; Dean, R. L., Bilsky, E. J., Negus, S. S., Eds.; Humana Press, c/o Springer Science + Business Media: New York, 2009.
3. Holtzman, S. G. *Life Sci.* **1979**, *24*, 219.
4. Frenk, H.; Rogers, G. H. *Behav. Neural Biol.* **1979**, *26*, 23.
5. Hadcock, J. R.; Scott, D. O. *Drug Discov. Today: Ther. Strateg.* **2005**, *2*, 171.
6. Lee, M. W.; Fujioka, K. *Expert Opin. Pharmacother.* **2009**, *10*, 1841.
7. Hausenloy, D. J. *Clin. Lipidol.* **2009**, *4*, 279.
8. Mitch, C. H.; Leander, J. D.; Mendelsohn, L. G.; Shaw, W. N.; Wong, D. T.; Cantrell, B. E.; Johnson, B. G.; Reel, J. K.; Snoddy, J. D.; Takemori, A. E.; Zimmerman, D. M. *J. Med. Chem.* **1993**, *36*, 2842.
9. Shaw, W. N. *Pharmacol. Biochem. Behav.* **1993**, *46*, 653.
10. Neary, P.; Delaney, C. P. *Expert Opin. Investig. Drugs.* **2005**, *14*, 479.
11. Portoghese, P. S. *J. Med. Chem.* **1965**, *8*, 609.
12. Fries, D. S. Opioid analgesics. In *Principles of Medicinal Chemistry*; Foye, W. O., Lemke, T. L., Williams, D. A., Eds.; Williams & Wilkins: Baltimore, 1995; p 453.
13. Wentland, M. P.; Lou, R.; Ye, Y.; Cohen, D. J.; Richardson, G. P.; Bidlack, J. M. *Bioorg. Med. Chem. Lett.* **2001**, *11*, 623.
14. Pedregal-Tercero, C.; Siegel, M. G.; Stucky, R. D.; Takeuchi, K. WO2004080968, 2004.
15. Blanco-Pillado, M.; Chappell, M. D.; Garcia De la Torre, M.; Diaz Buezo, N.; Fritz, J. E.; Holloway, W. G.; Matt, Jr., J. E.; Mitch, C. H.; Pedregal-Tercero, C.; Quimby, S. J.; Siegel, M. G.; Smith, D. R.; Stucky, R. D.; Takeuchi, K.; Thomas, E. M.; Wolfe, C. N. WO2004026305, 2004.
16. Pingali, S. R. K.; Madhav, M.; Jursic, B. S. *Tetrahedron Lett.* **2010**, *5*, 1383.
17. Balczewski, P.; Joule, J. A. *Synth. Commun.* **1990**, *20*, 2453.
18. [^{35}S]GTPgammaS binding assay measured by LEADseeker SPA (384 well): Dilute GTPgS^{35} 1:900 in assay buffer in half of required final assay volume (volume A). Add the corresponding standard agonist, Met-Enkephalin (hOPRD), Dynorphin A (hOPRK) or DAMGO (hOPRM) to give a solution concentration of 8× [EC_{50}], for a final assay concentration of 4× [EC_{50}] to volume A. Re-suspend LEADSeeker beads in assay buffer in order to generate a 40 mg/mL stock solution. GDP is dissolved in assay buffer at 1 mM. Add beads (100 μg/well final) to assay buffer containing saponin (60 μg/mL) in half of final assay volume (volume B). Mix well by vortexing. Add opioid membranes to each respective volume B, for a final assay concentration of 1.5 μg/well (hOPRD), 1.0 μg/well (hOPRK), and 1.5 μg/well (hOPRM). Continuously mix the bead/membrane solution (volume B) for 30 min prior to adding to the GTPgS^{35} solution (volume A) in a 1:1 ratio using a stir plate. Just prior to adding bead/membrane solution to the GTPgS^{35} solution, add GDP to volume B at 20 μM (10 μM final assay concentration). Add the bead/membrane solution to the GTPgS^{35} solution in a 1:1 ratio. Add 10 μL of the bead/membrane/GTPgS^{35} mix to the assay plate using a Multidrop (Titertek). Agitation of the solution is needed to prevent the beads/membrane from settling at the bottom. Plates are sealed, spun at 1000 rpm for 2 min, tapped on side to agitate and incubated at room temperature for 5 h. Plates are then imaged using a Viewlux Plus Imager (Perkin–Elmer).
19. Shiotani, S.; Kometani, T.; Iitaka, Y.; Itai, A. *J. Med. Chem.* **1978**, *21*, 153.
20. Fürst, S.; Hosztafi, S.; Friedmann, T. *Curr. Med. Chem.* **1995**, *1*, 423.
21. Zhang, A.; Xiong, W.; Bidlack, J. M.; Hilbert, J. E.; Knapp, B. I.; Wentland, M. P.; Neumeyer, J. L. *J. Med. Chem.* **2004**, *47*, 165.
22. Statnick, M. A.; Tinsley, F. C.; Eastwood, B. J.; Suter, T. M.; Mitch, C. H.; Heiman, M. L. *Am. J. Physiol. Regul. Integr. Comp. Physiol.* **2003**, *284*, 1399.
23. Schmidt, W. K. *Am. J. Surg.* **2001**, *182*, 27S.